Power strokes in molecular motors: Predictive, irrelevant, or somewhere in between?

Emanuele Penocchio,*,† Geyao Gu,† Alex Albaugh,‡ and Todd R. Gingrich*,†

†*Department of Chemistry, Northwestern University, 2145 Sheridan Road, Evanston, Illinois 60208, USA*

‡*Department of Chemical Engineering and Materials Science, Wayne State University, 5050 Anthony Wayne Drive, Detroit, Michigan 48202, USA*

E-mail: emanuele.penocchio@northwestern.edu; todd.gingrich@northwestern.edu

Abstract

For several decades, molecular motor directionality has been rationalized in terms of the free energy of molecular conformations visited before and after the motor takes a step, a so-called power-stroke mechanism with analogues in macroscopic engines. Despite theoretical and experimental demonstrations of its flaws, power-stroke language is quite ingrained, and some communities still value power-stroke intuition. By building a catalysis-driven motor into simulated numerical experiments, we here systematically report on how directionality responds when the motor is modified accordingly to power-stroke intuition. We confirm that the power stroke mechanism does not generally predict the directionality. Still, the relative stability of molecular conformations can nevertheless be a useful design element that helps one alter the directional bias of a molecular motor. The ostensible effectiveness of power-stroke intuition is explained by the recognition that to target conformation stability, one must alter interactions between moieties of a molecular motor, and those altered interactions do not affect the

power stroke in isolation. This can lead to apparent correlations between power stroke and directionality that one might leverage when engineering specific systems.

Introduction

Giving a preferred direction to the stochastic motion of molecules challenges our physical intuition, which is strongly informed by the macroscopic, deterministic regime.[1] At the nanoscale, inertial dynamics gives way to the randomness dance of Brownian motion, a dance that can be subtly biased to drift in one direction or another.[2] Living systems achieve directionality using molecular machinery[3] like kinesins,[4] dyneins,[5] and myosins,[6] processive motor proteins that move along microtubules in a preferred orientation. These autonomous motors are chemically driven by the hydrolysis of adenosine triphosphate (ATP) into adenosine diphosphate (ADP) and inorganic phosphate (P). Under physiological conditions, a thermodynamic driving force favors a net decomposition of ATP causing the motors to experience an environment with nonequilibrium concentrations of ATP, ADP, and P. By catalyzing ATP decomposition, the molecular motors couple their motion to the chemical driving force, transducing the free energy from the environment into directed motion.[7,8] Extensive experimental[9–19] and theoretical[7,20–23] studies have dissected mechanistic aspects of these processive motor proteins, leading to a comprehensive characterization of the chemistry underpinning their stochastic stride. One feature that is quite commonly observed (but by no means universal[24]) across the different architectures of these motor proteins is that the conformational changes allowing a motor to take a step are energetically downhill in the direction of motion.[17,25,26] These thermodynamically favored stepping reactions are frequently named "power strokes" and described as free-energy releasing, large-amplitude conformational changes.[27] The concept of power strokes is historically rooted in the study of the role of myosin in muscle contraction and was introduced to describe large structural changes in molecular motors performing mechanical work.[28,29] Pictorially, it has been de-

scribed as "the molecular analogue of an inclined plane".[30] Since the initial discussions of power strokes, many have focused on them as a feature necessary to generate a directional bias in molecular motors and perform work.[13,31–36] Power-stroke intuition has furthermore guided successful experimental efforts to reverse the direction of biological motors[37–41] and realize artificial light-driven motors.[42–45]

However, power strokes are known to be an incomplete and even problematic proxy for the directionality.[46–49] In short, theoretical arguments clarify that conformational changes yielding directed motion can be energetically uphill, downhill, or even flat, thus providing no information on directionality. Though the theoretical explanations are sound, it can be challenging for them to fully permeate given their abstractness and the apparent success of power strokes in explaining and engineering motors. Here, we set out to clarify why power strokes might serve as a design tool for engineering catalysis-driven motor performance even though they cannot be used to predict directionality in the absense of other information.[50]

Our approach leverages explicit coarse-grained simulations of a minimal-model motor[51] that was inspired by an experimentally realized motor.[52] In the last decade, chemists have designed such catalysis-driven motors as synthetic model systems[53–56] capable of probing the same fundamental principles of physics and chemistry that govern more complex protein motors.[47,50,57,58] The model systems[52,54] were designed without a "downhill" step. In other words, they specifically lack a power stroke, yet they realize directional motion via a mechanism known as a Brownian information ratchet.[59–61] By building that fundamental mechanism into simulated numerical experiments, we here report on how directionality responds when a power stroke feature, with variable strength, is added. In particular, we focus on the motor's bias, a measure of directionality quantifying the fraction of steps a motor takes in a specific direction.

Our work complements earlier efforts[46,47,50,62] to understand the relationship (or lack thereof) between power strokes and directionality in molecular motors and related systems. Kinetic models have already clarified that directionality only emerges when different motor

conformations have different catalytic properties, a condition known as kinetic asymmetry.[63–66] Based on these models, power strokes are *irrelevant*[46] for directionality, in that the kinetic asymmetry and hence the motor bias can run counter to the power stroke's orientation, a fact our simulations explicitly confirm. One might, however, naively misinterpret the irrelevance as a stronger claim: that introducing a power stroke into the motor chemistry would not affect the motor's bias. Our simulations clearly caution against that interpretation; adjusting the strength of the power stroke does alter the motor's bias. Within the regime where the changes to the power stroke and the resulting changes to the bias are correlated, one could utilize the power stroke as a design element to optimize a motor. One cannot expect those changes to be similarly correlated across all systems and all power stroke strengths. Indeed, our simulations explicitly show regimes within the same system in which larger power strokes yield more bias and regimes in which they yield less bias. Interestingly, however, we find that *within the regimes where the motor is fast* turning up the power stroke typically turns up the bias. This observation could explain why power strokes appear common throughout operational biological motors and why they have already been effectively used to engineer motors.

Results and Discussion

The model

We sought an explicit molecular dynamics model capturing the key features of a molecular motor[52] using the minimal set of physical ingredients leveraged by chemically-driven molecular machines in general, namely short- and long-range interactions, and Brownian motion.[2,47] As detailed in SI section 1.1, to build such a model, we coarse-grain moieties into volume-excluding spherical particles whose "chemical identity" is entirely determined by how they interact with each other. In essence, one can think of this model as a collection of particles which reciprocally attract and repel each other according to fixed potentials.

Those particles move in space with Langevin dynamics (see SI section 1.2) that incorporate (1) forces between the particles, (2) drag forces with an implicit solvent, and (3) random stochastic forces to mimic the thermal environment. Thanks to its coarse-grained character, our model can be simulated over time scales that are much longer than those afforded by classical all-atoms molecular dynamics simulations, which need enhanced sampling techniques to efficiently sample the timescales typical of molecular machines operation.[67,68] For illustrative purposes, we will color the particles according to their functional roles and use those colors to keep track of the different particle types.

As shown in Fig. 1a and described previously,[51] our classical model can explicitly simulate catalyzed coarse-grained chemical reactions. Consider a cluster of four blue particles bound along the edges of a tetrahedron encapsulating a single red particle, whose presence strains the blue tetrahedron. As a result, the filled tetrahedral cluster (FTC) is a metastable species – the stochastic dynamics eventually lead the red central particle (C) to escape, leaving an empty tetrahedral cluster (ETC).[69] These uncatalyzed decomposition events are rare as they require a large thermal fluctuation, but a patch of three white particles can catalyze this FTC $\rightleftharpoons$ ETC + C reaction. As shown in Fig. 1a (bottom), when an FTC gets close enough, interactions with the white particles stretch the blue particles enough for the red C to escape and bind to the white particles. The typical mechanism for the catalyzed FTC decomposition thus proceeds via a long-lived intermediate where a C particle binds to the catalytic unit and eventually leaves. This mechanism can be thought of as a continuous, microscopically reversible version of the Michaelis-Menten scheme executed explicitly within a molecular dynamics simulation.

Akin to how biological motors are coupled to ATP decomposition, the FTC $\rightleftharpoons$ ETC + C reaction couples to the catenane motor shown in Fig. 1b. Briefly, we choose interparticle potentials (see SI section 1.1) so that black particles form a stable circular track around which moves a shuttling ring built from green particles. That green ring feels an attraction to two different orange particles, binding sites, located on opposing sides of the black track.

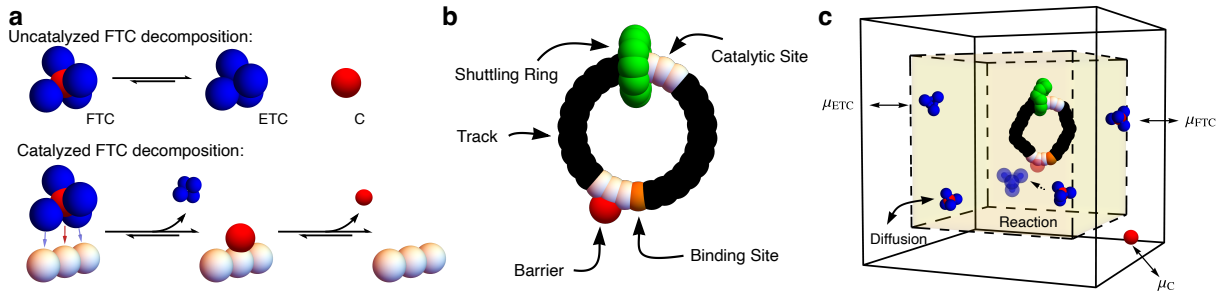

Figure 1: A catalysis-driven motor simulated explicitly with coarse-grained molecular dynamics. **a**, Coarse-grained catalysis. The uncatalyzed escape (top) of a bulky red particle (C) from a full tetrahedral cluster (FTC) is thermodynamically favored, as the blue particles experience strong harmonic bond interactions (see SI section 1.1) that make the empty tetrahedral cluster (ETC) the most stable configuration. The process is faster in presence of a catalytic unit (bottom) constituted by a patch of three white particles interacting with blue and red particles. **b**, Structure of the coarse-grained motor. A ring of particles (green) can freely diffuse along a track (black) incorporating two binding sites (orange) when its path is not hindered by a barrier (red). The latter can form as long-lived intermediates during FTC decomposition catalyzed by either catalytic unit. **c**, Simulation box. As detailed in SI section 1.2.1, a periodic-boundary-condition simulation box is divided into a motor-containing region (yellow), where particles move according to Langevin dynamics, and an exterior region (white), where the Langevin dynamics are supplemented with grand canonical Monte Carlo chemostats holding FTC, ETC, and C species at fix chemical potentials μ_{FTC}, μ_{ETC}, and μ_{C}, respectively, such that $\mu_{\mathrm{FTC}} - \mu_{\mathrm{ETC}} - \mu_{\mathrm{C}} > 0$. This setup allows simulating the motor under nonequilibrium conditions associated with a surplus of FTC (see SI for movies depicting representative simulations).

Finally, two catalytic units are placed next to the binding sites.

Two sources of asymmetry are worth noting. The first is a structural asymmetry (or anisotropy[56]) in the motor's design, where catalytic sites are placed just to the clockwise side of the binding sites. The second is kinetic asymmetry,[63–65] which arises because, when the ring sits on a binding site, it hinders the proximal catalytic site. Consequently, the rate of catalysis, and therefore the rate at which red particles bind to catalytic sites, depends on the position of the ring. Structural and kinetic asymmetry are together necessary and sufficient conditions to generate directional bias by harnessing fluctuations in chemical nonequilibrium conditions. Indeed, a functional motor emerges when the reaction is held out of equilibrium by the injection of FTC and removal of ETC and C, achieved in our case by chemostats that preserve a chemical potential difference between the FTC, ETC, and C species, namely $\mu_{\mathrm{FTC}} - \mu_{\mathrm{ETC}} - \mu_{\mathrm{C}} > 0$, as illustrated in Fig. 1. Our prior work has demonstrated that the resulting model explicitly couples the FTC $\rightleftharpoons$ ETC + C reaction to drive steady-state current of the shuttling ring, displaying similar kinetic relations to processes in experimental motors (e.g., shuttling is much faster than catalysis).[51] We have also shown that the mean current can be flipped between the clockwise and counter-clockwise orientation with structural changes,[70] and statistical fluctuations in the current decrease with increasing FTC consumption.[71]

Introducing a power stroke

The simulations allow us to measure how nonequilibrium steady-state dynamical behavior, most notably the motor's directional bias (the fraction of ring's cycles in a specific direction) and current (the net cycling rate), depends on the interactions between motor moieties. In the present work, we focus on how the motor's performance depends on the introduction of a power stroke, achieved by setting the strength of interactions between red barriers and green ring particles. To see that this interaction introduces a power stroke, it is useful to recapitulate the basic mechanism of this class of catenane motors. The shuttling ring

executes a random walk in which it dwells at one orange binding site before taking a rare hop to the other binding site. This hop, initiated by a thermal fluctuation, can proceed in the clockwise or counter-clockwise direction. However, if a red C particle is bound to a white catalytic site, it acts as a barrier, blocking the ring from moving in that direction. If both catalytic sites are blocked, the ring cannot hop from one binding site to the other. If none are blocked, there can be no preferred direction. Motion with a directed bias requires a barrier on one side but not the other, thus making the two conformations of Fig. 2a particularly important. One of those conformations has the green shuttling ring proximal to the red C and the other conformation has those two far enough apart that they do no interact. Because of the structural asymmetry, transitioning from the proximal to distal conformation requires the ring to move counter-clockwise while a distal-to-proximal transition requires clockwise rotation. Kinetic asymmetry promotes the distal conformation over the proximal one, disfavouring barrier formation on the catalytic site close to the ring. The resulting population imbalance is what ultimately creates directionality by making distal-to-proximal jumps more frequent than proximal-to-distal. Power-stroke intuition would suggest that one could drive the motion more strongly in the clockwise direction if the free energy of the proximal configuration is lowered to stabilize that state, thus making distal-to-proximal jumps more "irreversible".

Within our simulation model, it is straightforward to adjust the interactions between red and green particles, allowing us to both stabilize and destabilize that proximal state as sketched in Fig. 2a. This is because the model includes a set of Lennard-Jones pair potentials determining how one specific kind of particle attracts or repels the others:

$$U_{\mathrm{Lennard-Jones}}(\boldsymbol{r}) = 4\epsilon_R \left(\frac{\sigma}{|\boldsymbol{r}|}\right)^{12} - 4\epsilon_A \left(\frac{\sigma}{|\boldsymbol{r}|}\right)^{6}, \tag{1}$$

where $\boldsymbol{r}$ is the distance between the particles, σ is their volume-exclusion radius, and ϵ_R and ϵ_A are respectively the strengths of steric (short-ranged) and long-ranged interactions

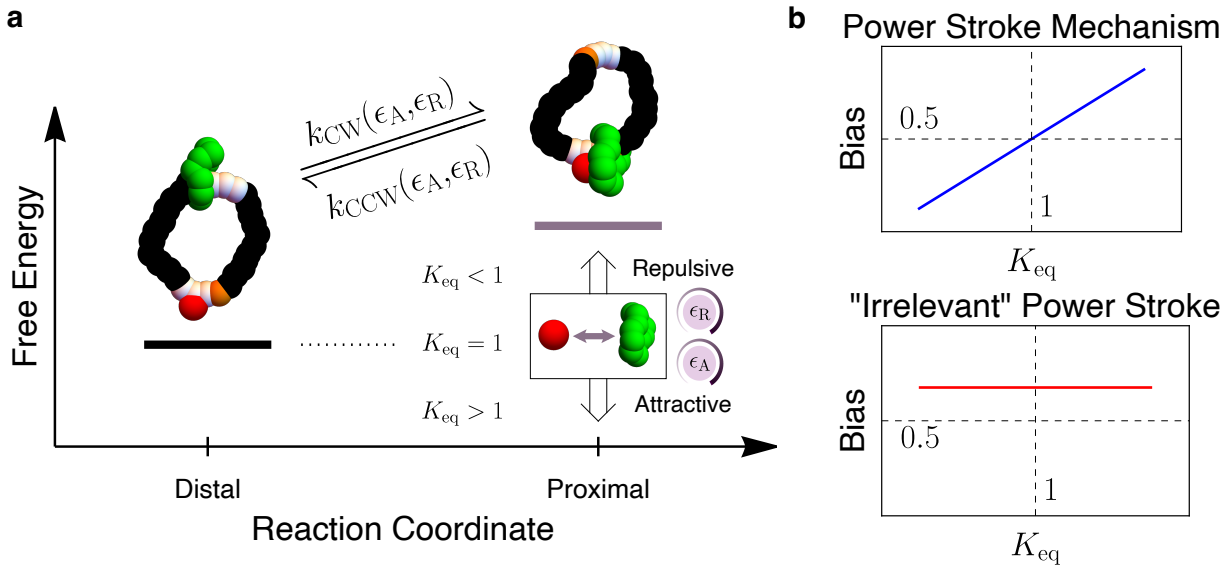

Figure 2: Modelling the power stroke. **a**, Sketch of how the power stroke can be tuned in our simulation model. By varying the steric repulsion (ϵ_R) and the long-range attraction (ϵ_A) parameters between the green ring and the red barrier in Equation 1, the thermodynamic stability of the proximal conformation with respect to the distal one can be arbitrarily varied, thus tuning the magnitude of the power stroke, quantified by K_{eq}. The average rate for transitioning between the two conformations (k_{CW} and k_{CCW}) will vary accordingly and can be directly extracted from steady-state simulations. **b**, Hypothesized responses to varying proximal conformation free energy. According to the power stroke mechanism (top), the free energy difference between distal and proximal conformations dictate directionality, and the motor's bias (as defined in Eq. (3)) increases monotonically with K_{eq}, being 0.5 when $K_{eq} = 1$ as neither conformation is thermodynamically favored. Kinetic models[46,50] (bottom) have clarified that the motor bias would not change if the free energy of motor conformations were varied in isolation, i.e., without affecting transition state free energies. In this scenario (discussed as "Case 2" in Ref[50]), varying the power stroke is irrelevant to the bias value. Consequently, deviations from this behavior are signatures that the free energy of motor conformations are not varied in isolation.

between red and green particles that can be tuned independently in our simulations. In our model, the particles are always bulky ($\epsilon_R > 0$) and long-range interactions can be either zero ($\epsilon_A = 0$) or attractive ($\epsilon_A \geq 0$). We can translate from the interaction strengths (ϵ_R and ϵ_A) into the chemical language of an equilibrium constant since

$$K_{\mathrm{eq}}(\epsilon_R, \epsilon_A) = \frac{[\mathrm{proximal}]_{\mathrm{eq}}}{[\mathrm{distal}]_{\mathrm{eq}}}, \tag{2}$$

which is an effective quantification of the power stroke. Though we tune both ϵ_R and ϵ_A in our numerical experiments, we can extract the resulting $K_{\mathrm{eq}}(\epsilon_R, \epsilon_A)$ and thereafter focus our attention on how the motor performance depends on it. $K_{\mathrm{eq}} = 1$ corresponds to degenerate proximal and distal states—no power stroke as in Ref.,[52] while $K_{\mathrm{eq}} > 1$ corresponds to a power stroke in the clockwise direction. By making the green and red particles strongly repulsive, we can additionally induce a power stroke in the counter-clockwise direction with $K_{\mathrm{eq}} < 1$. In synthetic terms, varying ϵ_A or ϵ_R can be qualitatively thought of as allowing the formation of a complex that binds the barrier and the macrocycle or as varying the steric bulk of the barrier, respectively. Such strategies to experimentally introduce a power stroke in the motor have been previously proposed[72,73] and are here explicitly built into simulated numerical experiments.

Motor bias as a function of K_{eq}

For each green-red interaction strength, we simulated motors under the nonequilibrium conditions and counted the number of clockwise (n_{CW}) and counterclockwise (n_{CCW}) cycles performed by the ring once the system has reached the steady state. The clockwise bias,

$$\mathrm{bias} = \frac{n_{\mathrm{CW}}}{n_{\mathrm{CW}} + n_{\mathrm{CCW}}} \tag{3}$$

is a measure of the fraction of completed cycles in the clockwise direction, so a bias of 0.5 implies no directionality. If the power stroke were a generic determinant of the motor's

direction, one would expect the bias to be 0.5 when $K_{eq} = 1$. Furthermore, one would anticipate that the bias climbs above 0.5 when $K_{eq} > 1$ (favors proximal) and drops below 0.5 when $K_{eq} < 1$ (favors distal), as in Fig. 2b (top). We did not expect that power-stroke prediction because we know from kinetic models that kinetic asymmetry is the ultimate driver of directionality. Even with the identification of kinetic asymmetry as the driver, however, it is not straightforward to anticipate how the kinetic asymmetry (and hence the bias) would correlate with K_{eq}. The answer depends on *how* one varies K_{eq}.

One might consider a kinetic model in which *only* the free energy of that proximal state is affected by the introduction of the power stroke and the free energies of all other states and transition states remain unaffected. In that scenario, K_{eq} would be tuned accordingly, and yet kinetic models make clear that the bias would not be affected.[46,72] In graphical terms, the bias would be flat as a function of K_{eq}, as in Fig. 2b (bottom). However, it is not particularly physical to independently vary the free energy of a single state. A power of our *simulation* model as compared to *kinetic* chemical reaction network models is that we are introducing energetic interactions between moieties, not just changing the energies of isolated states in a network model. By directly controlling interaction energies, we change the motor in the same sort of way one might in a real experiment (e.g., make a moiety bulkier, more charged, etc.). One might adjust those interactions with the explicit goal of changing, say, the proximal state's free energy, but other energies could also shift as a side effect. For instance, when the attraction between the ring and the barrier is tuned up in our simulation model, it has the effect of increasing the power stroke as visualized in Fig. 2a, but it also decreases the rate for a red C particle to detach from the catalytic site in the proximal conformation, altering the kinetic asymmetry, and thus the bias, as a side effect. Our model naturally captures those side effects, which can allow power stroke engineering to alter the motor's bias.

Fig. 3a-b (top) shows that the bias responds nontrivially to changes in the power stroke. In agreement with the theoretical arguments,[46] the data illustrate that the power stroke

direction does not generically align with the bias. Fig. 3a (top), for example, shows clockwise bias whether K_{eq} is greater than or less than 1. At the same time, the data show altering the power stroke is not irrelevant in that the bias changes when K_{eq} is tuned. The particular way the bias varies with K_{eq} depends on how K_{eq} is adjusted, either through ϵ_R or ϵ_A. For three different fixed strengths of barrier repulsion, we adjusted the attractions from weakly attractive to strongly attractive so as to drive from $K_{\mathrm{Eq}} \ll 1$ to $K_{\mathrm{Eq}} \gg 1$, revealing the bias to be essentially insensitive to the repulsion strength (see Fig. 3a (top)). However, for a fixed attraction strength, there is a threshold at which the repulsion (i.e., barrier's bulkiness) becomes so weak that the ring can pass over a barrier, thus causing the motor bias to collapse and even go negative (Fig. 3b (top)).

Power strokes as an engineering tool

We have shown simulation results that explicitly illustrate a situation in which the power stroke does not align with the directional bias; the bias exceeds 0.5 even when K_{eq} is less than one. One may, nevertheless, ask if some differential version of power-stroke intuition can hold, namely if making the power stroke more strongly downhill to the right actually makes the bias push more strongly to the right. From an engineering perspective, it would be appealing to observe strong correlations between the change in power stroke and the change in bias. Such a correlation would reflect that one can anticipate how the bias would change by tuning the K_{eq} that regulates how probability partitions between only two states. Since a change in interaction energies between pairs of moeities simultaneously shifts energies of many states, it is a tremendous simplification if one can reason about the motor by focusing only on the two states involved in a power stroke. The nonmonotonic dependence of the bias on K_{eq} in Fig. 3 reflects that simplification cannot broadly hold because there are regimes in which pushing K_{eq} harder to the right decreases the rightward bias. Nevertheless, the simplification can apply within the monotonically increasing regimes observed in the top plots of Fig. 3a-b, and we observe those regimes align with the parameter regimes that yield

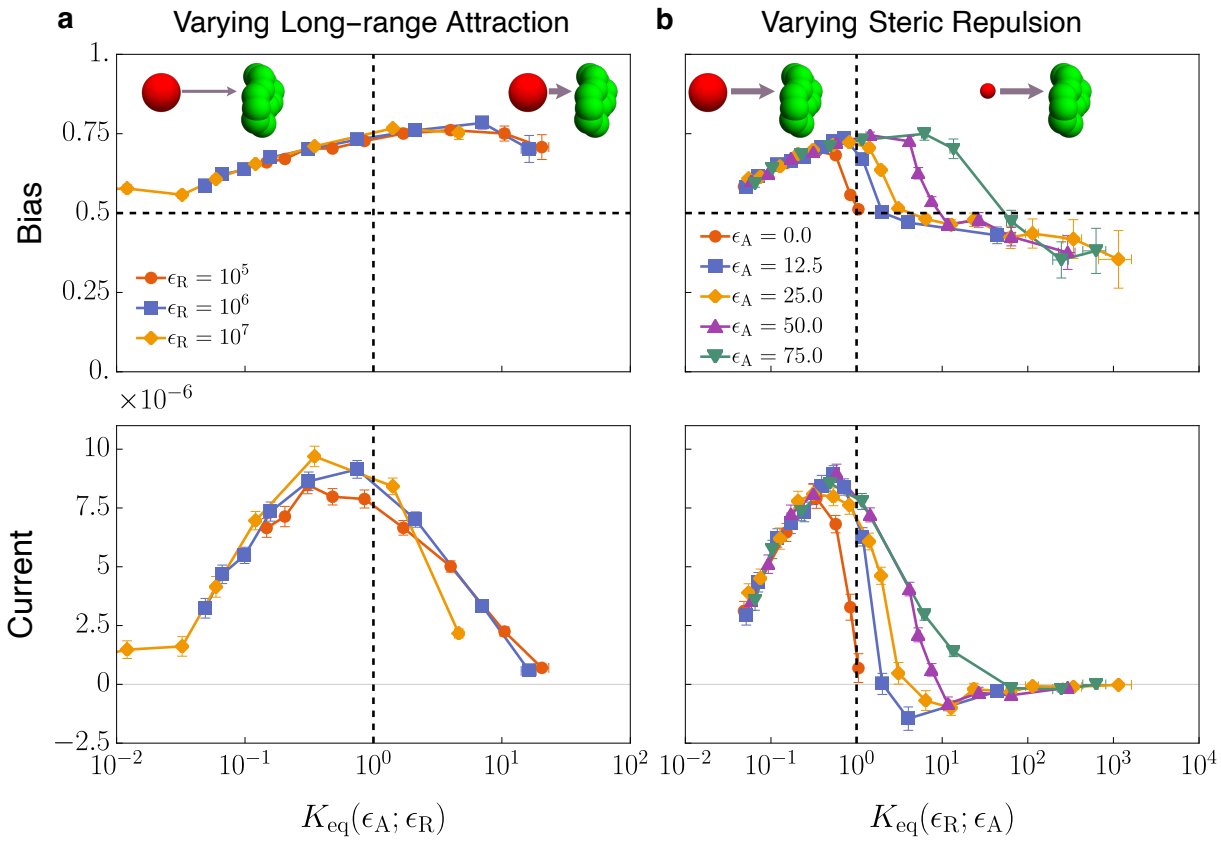

Figure 3: The effect of altering power stroke. Each data point was obtained by averaging over 100 independent simulations of motor designs with different values of the attraction (ϵ_A) and repulsion (ϵ_R) parameters defining the interaction between green ring and red barrier particles in equation (1). All the other parameters are set to their default values as in Ref.[51] (reference parameters correspond to "Motor II" in that study). Bias and current are computed from simulations data according to equations (3) and (4), respectively. As indicated in the plot legends, colored lines connect motor designs with the same ϵ_A or ϵ_R, with the unshared parameter being varied along the horizontal axis thus tuning K_{eq}. SI sections 2.1 and 2.2 provide a detailed explanation of K_{eq} calculation and a full rationalization of the plots based on the model physical ingredients, respectively. **a**, Motor's directional bias (top) and current (bottom) obtained by varying ϵ_A for fixed values of ϵ_R. **b**, Motor's directional bias (top) and current (bottom) obtained by varying ϵ_R for fixed values of ϵ_A.

high-current motors.

To make this claim, we compute

$$\text{current} = \frac{n_{\text{CW}} - n_{\text{CCW}}}{t_{\text{obs}}}\,, \tag{4}$$

where t_{obs} is the observed simulation time. Fig. 3a-b (bottom) shows that current versus K_{eq}, demonstrating the alignment—the values of K_{eq} that give high-current motors are precisely the same values that give a monotonically increasing bias-K_{eq} relation. This alignment suggests that, at least within this model, the functional (high-current) motors are also the ones for which the power-stroke intuition could offer an engineering benefit. Within this fast-motor regime, turning up the power stroke indeed turns up the bias. These observations could provide an explanation for why power-stroke engineering can sometimes work even though power strokes do not generically determine directionality. Given the starting point of a functional motor, found by evolution or designed cleverly, our model suggests that regimes might exist where the change in that motor's bias may well be anticipated by adjusting the power stroke. On a side note, the bottom plots in Fig. 3a-b are consistent with experimental observations that currents in enzyme catalysis are optimized when all the states in a catalytic mechanism have more or less the same free energy ($K_{\text{eq}} \approx 1$).[74] This is no surprise, as the motor is ultimately a catalyst for FTC decomposition, and reiterates that our minimal model well reproduces features observed in real chemical systems.

Metastability, coarse graining, and the quantification of power strokes

The power stroke idea centers around an identification of only two important conformations, one visited before and one after a motor's processive step. It was introduced to explain the nonequilibrium dynamics in terms of K_{eq}, which expresses how probability partitions between those two states in a dynamic *equilibrium* (see Eq. (2)). The quantification of that K_{eq} involves some nuance because it presupposes that the two macrostates, corresponding, say, to

distal and proximal conformations, can be cleanly defined. That definition involves averaging over many microscopic states, each of which is classified as one of the two macrostates. In general, it is challenging to precisely group many microstates into macrostates, but we are focused on situations with extreme timescale separation—a ring metastably stays on a binding site for long times before transiting to the other site relatively quickly. That timescale separation makes classification more clear cut. Experimentally, the distal conformation may contribute a particular NMR peak and the proximal another peak, such that K_{eq} is extracted as the ratio of peaks in equilibrium.[52–54,62] In the simulations, we must introduce a grouping procedure for sorting microstates into the distal and proximal macrostates. While different reasonable choices can subtly alter the quantification of K_{eq}, our results are practically insensitive to minor ambiguities defining the boundary of the macrostates. This insensitivity emerges for two reasons: shifting all points in Fig. 3 left or right by small amounts does not alter the essential shape of the curves, and besides, small variation in how K_{eq} is quantified becomes undetectable when K_{eq} is naturally viewed on a logarithmic scale.

While Eq. 2 defines K_{eq} in terms of equilibrium populations of the distal and proximal macrostates, because equilibrium obeys detailed balance, K_{eq} can equivalently be cast as a ratio of kinetic rate constants $K_{\mathrm{eq}} = k_{\mathrm{CW}}/k_{\mathrm{CCW}}$. Because our simulations involve chemostats which hold the system away from equilibrium, the latter formulation is particularly convenient as those rate constants can be extracted directly from the nonequilibrium simulations. In practice, as detailed in SI section 2.1, we extract the rate constants by counting how many transitions per unit time are observed between the states shown in Fig. 2a.

As we have discussed, a shortcoming of the power stroke framing is that it focuses only on two coarse-grained states. Our results confirm that the mechanism of the motor and its directionality simply cannot be deduced from only those two states. Rather, the motor's mechanism is better reflected by coarse graining the kinetics into a more complete Markov model that introduces more states to account for barrier addition and removal events. In SI section 2.3, we discuss how a Markov model with only 16 states is sufficient to rationalize

the changes to motor performance plotted in Fig. 3.

Conclusion

We have provided a resolution to a molecular motor conundrum. On the one hand, power strokes are observed in nature, have been used by many to explain directionality in molecular motors, and provided practical intuition for engineering attempts. On the other hand, kinetic models clearly show that power strokes cannot determine directionality, and synthetic motors lacking power strokes have been successfully designed. Kinetic models also show that one should expect the motor's directionality to be unaltered by changing the thermodynamic stability of its conformations, overlooking power-stroke engineering. Our simulation-based approach confirms that the power stroke mechanism cannot predict the directionality of a catalysis-driven motor, which is, in fact, determined by structural and kinetic asymmetry through an information ratchet mechanism. At the same time, our explicit model displays regimes where changes to the motor's bias correlate with changes to the power stroke magnitude. It is, therefore, possible that similar correlations are present in biological motors that have been optimized throughout evolution. This might justify the apparent effectiveness of the power stroke intuition in its differential version, which is the basis of successful engineering experiments on biological motors.

The work suggests that introducing power strokes in chemically-driven synthetic molecular motors might increase or decrease their directional bias, thus providing a practical way to alter kinetic asymmetry in Brownian information ratchets. This suggestion is somewhat in contrast with the understanding provided by kinetic models,[73] that accounts for a similar behaviour only in those light-driven motors implementing a power-stroke mechanism[44,45] or in energy ratchets.[61,75] We come to a different conclusion because our simulation model captures additional aspects of the physics which are hard to a priori build into kinetic models. We could extract a kinetic model from the simulations that captures those effects, but this requires knowledge of how design modifications impact all the kinetic rate constants in

the model. By mimicking experiments more directly, our simulation model naturally captures these side effects and could be used to assess the effect of those design modifications. We conclude that experimental data aligning with power-stroke intuition are possible and accounted for by the Brownian ratchet mechanism and the concept of kinetic asymmetry. However, no general principles apply to power-stroke intuition in catalysis-driven systems and predicting when and how introducing power strokes might help engineering motors requires system-specific studies. Generalizing our molecular dynamics approach to explicitly simulate far from equilibrium chemical systems, even beyond molecular motors, can be of great help for the field, complementing kinetic models.

Acknowledgements

We thank Shuntaro Amano, Raymond D. Astumian, Stefan Borsley, David A. Leigh and Ben M.W. Roberts for useful discussions and comments on early versions of the manuscript. We acknowledge support from the Gordon and Betty Moore Foundation (Grant No. GBMF10790 to T.R.G.)

Supporting Information Available: The Supporting Information is available free of charge.

References

(1) Feynman, R. P.; Leighton, R. B.; Sands, M. *The Feynman lectures on physics*; Addison–Wesley, 1964; Vol. I, Chap. 46.

(2) Astumian, R. D.; Hänggi, P. Brownian motors. *Phys. Today* **2002**, *55*, 33–39.

(3) Schliwa, M., Ed. *Molecular Motors*; Wiley-VCH, 2003.

(4) Block, S. M. Kinesin Motor Mechanics: Binding, Stepping, Tracking, Gating, and Limping. *Biophys. J.* **2007**, *92*, 2986-2995.

(5) Bhabha, G.; Johnson, G. T.; Schroeder, C. M.; Vale, R. D. How Dynein Moves Along Microtubules. *Trends Biochem. Sci.* **2015**, *41*, 94-105.

(6) Robert-Paganin, J.; Pylypenko, O.; Kikuti, C.; Sweeney, H. L.; Houdusse, A. Force Generation by Myosin Motors: A Structural Perspective. *Chem. Rev.* **2020**, *120*, 5–35.

(7) Mugnai, M. L.; Hyeon, C.; Hinczewski, M.; Thirumalai, D. Theoretical perspectives on biological machines. *Rev. Mod. Phys.* **2020**, *92*, 025001.

(8) Brown, A. I.; Sivak, D. A. Theory of Nonequilibrium Free Energy Transduction by Molecular Machines. *Chem. Rev.* **2020**, *120*, 434–459.

(9) Sablin, E. P.; Case, R. B.; Dai, S. C.; Hart, C. L.; Ruby, A.; Vale, R. D.; Fletterick, R. J. Direction determination in the minus-end-directed kinesin motor ncd. *Nature* **1998**, *395*, 813–816.

(10) Rice, S.; Lin, A. W.; Safer, D.; Hart, C. L.; Naber, N.; Carragher, B. O.; Cain, S. M.; Pechatnikova, E.; Wilson-Kubalek, E. M.; Whittaker, M.; Pate, E.; Cooke, R.; Taylor, E. W.; Milligan, R. A.; Vale, R. D. A structural change in the kinesin motor protein that drives motility. *Nature* **1999**, *402*, 778–784.

(11) Mehta, A. D.; Rock, R. S.; Rief, M.; Spudich, J. A.; Mooseker, M. S.; Cheney, R. E. Myosin-V is a processive actin-based motor. *Nature* **1999**, *400*, 590–593.

(12) Rock, R. S.; Rice, S. E.; Wells, A. L.; Purcell, T. J.; Spudich, J. A.; Sweeney, H. L. Myosin VI is a processive motor with a large step size. *Proc. Natl. Acad. Sci. USA* **2001**, *98*, 13655–13659.

(13) Howard, J. *Mechanics of Motor Proteins and the Cytoskeleton*; Oxford University Press, Oxford, 2001.

(14) Yildiz, A.; Tomishige, M.; Vale, R. D.; Selvin, P. R. Kinesin Walks Hand-Over-Hand. *Science* **2004**, *303*, 676–678.

(15) Reck-Peterson, S. L.; Yildiz, A.; Carter, A. P.; Gennerich, A.; Zhang, N.; Vale, R. D. Single-Molecule Analysis of Dynein Processivity and Stepping Behavior. *Cell* **2006**, *126*, 335–348.

(16) Toba, S.; Watanabe, T. M.; Yamaguchi-Okimoto, L.; Toyoshima, Y. Y.; Higuchi, H. Overlapping hand-over-hand mechanism of single molecular motility of cytoplasmic dynein. *Proc. Natl. Acad. Sci. USA* **2006**, *103*, 5741–5745.

(17) Hyeon, C.; Klumpp, S.; Onuchic, J. N. Kinesin's backsteps under mechanical load. *Phys. Chem. Chem. Phys.* **2009**, *11*, 4899–4910.

(18) Andrecka, J.; Ortega Arroyo, J.; Takagi, Y.; de Wit, G.; Fineberg, A.; MacKinnon, L.; Young, G.; Sellers, J. R.; Kukura, P. Structural dynamics of myosin 5 during processive motion revealed by interferometric scattering microscopy. *eLife* **2015**, *4*, e05413.

(19) Ariga, T.; Tomishige, M.; Mizuno, D. Nonequilibrium Energetics of Molecular Motor Kinesin. *Phys. Rev. Lett.* **2018**, *121*, 218101.

(20) Jülicher, F.; Ajdari, A.; Prost, J. Modeling molecular motors. *Rev. Mod. Phys.* **1997**, *69*, 1269–1282.

(21) Liepelt, S.; Lipowsky, R. Kinesin's Network of Chemomechanical Motor Cycles. *Phys. Rev. Lett.* **2007**, *98*, 258102.

(22) Kolomeisky, A. B.; Fisher, M. E. Molecular Motors: A Theorist's Perspective. *Annu. Rev. Phys. Chem.* **2007**, *58*, 675–695.

(23) Takaki, R.; Mugnai, M. L.; Thirumalai, D. Information flow, gating, and energetics in dimeric molecular motors. *Proc. Natl. Acad. Sci. U.S.A.* **2022**, *119*, e2208083119.

(24) Mukherjee, S.; Warshel, A. Electrostatic origin of the unidirectionality of walking myosin V motors. *Proc. Natl. Acad. Sci. U.S.A.* **2013**, *110*, 17326–17331.

(25) Hyeon, C.; Onuchic, J. N. Mechanical control of the directional stepping dynamics of the kinesin motor. *Proc. Natl. Acad. Sci. U.S.A.* **2007**, *104*, 17382–17387.

(26) Lin, J.; Okada, K.; Raytchev, M.; Smith, M. C.; Nicastro, D. Structural mechanism of the dynein power stroke. *Nat. Cell Biol.* **2014**, *16*, 479–485.

(27) Howard, J. Protein power strokes. *Curr. Biol.* **2006**, *16*, R517.

(28) Huxley, H. E. The Mechanism of Muscular Contraction. *Science* **1969**, *164*, 1356–1366.

(29) Huxley, A. F.; Simmons, R. M. Proposed Mechanism of Force Generation in Striated Muscle. *Nature* **1971**, *233*, 533–538.

(30) Bustamante, C.; Keller, D.; Oster, G. The Physics of Molecular Motors. *Acc. Chem. Res.* **2001**, *34*, 412–420.

(31) Eisenberg, E.; Hill, T. L. A cross-bridge model of muscle contraction. *Prog. Biophys. Mol. Biol.* **1979**, *33*, 55–82.

(32) Eisenberg, E.; Hill, T.; Chen, Y. Cross-bridge model of muscle contraction. Quantitative analysis. *Biophys. J.* **1980**, *29*, 195–227.

(33) Spudich, J. A. The myosin swinging cross-bridge model. *Nat. Rev. Mol. Cell Biol.* **2001**, *2*, 387–392.

(34) Wang, H.; Oster, G. Ratchets, power strokes, and molecular motors. *Appl. Phys. A* **2002**, *75*, 315–323.

(35) Wagoner, J. A.; Dill, K. A. Molecular Motors: Power Strokes Outperform Brownian Ratchets. *J. Phys. Chem. B* **2016**, *120*, 6327–6336.

(36) Hwang, W.; Karplus, M. Structural basis for power stroke vs. Brownian ratchet mechanisms of motor proteins. *Proc. Natl. Acad. Sci. U.S.A.* **2019**, *116*, 19777–19785.

(37) Tsiavaliaris, G.; Fujita-Becker, S.; Manstein, D. J. Molecular engineering of a backwards-moving myosin motor. *Nature* **2004**, *427*, 558–561.

(38) Bryant, Z.; Altman, D.; Spudich, J. A. The power stroke of myosin VI and the basis of reverse directionality. *Proc. Natl. Acad. Sci. U.S.A.* **2007**, *104*, 772–777.

(39) Liao, J.-C.; Elting, M. W.; Delp, S. L.; Spudich, J. A.; Bryant, Z. Engineered Myosin VI Motors Reveal Minimal Structural Determinants of Directionality and Processivity. *J. Mol. Biol.* **2009**, *392*, 862–867.

(40) Chen, L.; Nakamura, M.; Schindler, T. D.; Parker, D.; Bryant, Z. Engineering controllable bidirectional molecular motors based on myosin. *Nat. Nanotechnol.* **2012**, *7*, 252–256.

(41) Can, S.; Lacey, S.; Gur, M.; Carter, A. P.; Yildiz, A. Directionality of dynein is controlled by the angle and length of its stalk. *Nature* **2019**, *566*, 407–410.

(42) Koumura, N.; Zijlstra, R. W. J.; van Delden, R. A.; Harada, N.; Feringa, B. L. Light-driven monodirectional molecular rotor. *Nature* **1999**, *401*, 152–155.

(43) Conyard, J.; Addison, K.; Heisler, I. A.; Cnossen, A.; Browne, W. R.; Feringa, B. L.; Meech, S. R. Ultrafast dynamics in the power stroke of a molecular rotary motor. *Nat. Chem.* **2012**, *4*, 547–551.

(44) Astumian, R. D. Optical vs. chemical driving for molecular machines. *Faraday Discuss.* **2016**, *195*, 583–597.

(45) Astumian, R. D. Kinetic Asymmetry and Directionality of Nonequilibrium Molecular Systems. *Angew. Chem. Int. Ed.* **2024**, *63*, e202306569.

(46) Astumian, R. D. Irrelevance of the Power Stroke for the Directionality, Stopping Force, and Optimal Efficiency of Chemically Driven Molecular Machines. *Biophys. J.* **2015**, *108*, 291–303.

(47) Astumian, R. D.; Mukherjee, S.; Warshel, A. The Physics and Physical Chemistry of Molecular Machines. *ChemPhysChem* **2016**, *17*, 1719–1741.

(48) Mukherjee, S.; Alhadeff, R.; Warshel, A. Simulating the dynamics of the mechanochemical cycle of myosin-V. *Proc. Natl. Acad. Sci. USA* **2017**, *114*, 2259–2264.

(49) Alhadeff, R.; Warshel, A. Reexamining the origin of the directionality of myosin V. *Proc. Natl. Acad. Sci. USA* **2017**, *114*, 10426–10431.

(50) Amano, S.; Esposito, M.; Kreidt, E.; Leigh, D. A.; Penocchio, E.; Roberts, B. M. W. Using Catalysis to Drive Chemistry Away from Equilibrium: Relating Kinetic Asymmetry, Power Strokes, and the Curtin–Hammett Principle in Brownian Ratchets. *J. Am. Chem. Soc.* **2022**, *144*, 20153–20164.

(51) Albaugh, A.; Gingrich, T. R. Simulating a chemically fueled molecular motor with nonequilibrium molecular dynamics. *Nat. Commun.* **2022**, *13*, 2204.

(52) Wilson, M. R.; Solà, J.; Carlone, A.; Goldup, S. M.; Lebrasseur, N.; Leigh, D. A. An autonomous chemically fuelled small-molecule motor. *Nature* **2016**, *534*, 235–240.

(53) Borsley, S.; Leigh, D. A.; Roberts, B. M. W. A Doubly Kinetically-Gated Information Ratchet Autonomously Driven by Carbodiimide Hydration. *J. Am. Chem. Soc.* **2021**, *143*, 4414–4420.

(54) Borsley, S.; Kreidt, E.; Leigh, D. A.; Roberts, B. M. W. Autonomous fuelled directional rotation about a covalent single bond. *Nature* **2022**, *604*, 80–85.

(55) Borsley, S.; Leigh, D. A.; Roberts, B. M. W. Tuning the force, speed, and efficiency of an autonomous chemically fueled information ratchet. *J. Am. Chem. Soc.* **2022**, *144*, 17241–17248.

(56) Borsley, S.; Leigh, D.; Roberts, B. M. W. Molecular Ratchets and Kinetic Asymmetry: Giving Chemistry Direction. *Angew. Chem. Int. Ed. n/a*, e202400495.

(57) Amano, S.; Borsley, S.; Leigh, D. A.; Sun, Z. Chemical engines: driving systems away from equilibrium through catalyst reaction cycles. *Nat. Nanotechnol.* **2021**, *16*, 1057–1067.

(58) Borsley, S.; Leigh, D. A.; Roberts, B. M. W. Chemical fuels for molecular machinery. *Nat. Chem.* **2022**, *14*, 728–738.

(59) Astumian, R. D.; Derényi, I. Fluctuation driven transport and models of molecular motors and pumps. *European Biophysics Journal* **1998**, *27*, 474–489.

(60) Kay, E. R.; Leigh, D. A.; Zerbetto, F. Synthetic Molecular Motors and Mechanical Machines. *Angew. Chem. Int. Ed.* **2007**, *46*, 72–191.

(61) Sangchai, T.; Al Shehimy, S.; Penocchio, E.; Ragazzon, G. Artificial Molecular Ratchets: Tools Enabling Endergonic Processes. *Angew. Chem. Int. Ed. n/a*, e202309501.

(62) Binks, L.; Borsley, S.; Gingrich, T. R.; Leigh, D. A.; Penocchio, E.; Roberts, B. M. W. The role of kinetic asymmetry and power strokes in an information ratchet. *Chem* **2023**, *9*, 2902–2917.

(63) Astumian, R. D.; Chock, P. B.; Tsong, T. Y.; Westerhoff, H. V. Effects of oscillations and energy-driven fluctuations on the dynamics of enzyme catalysis and free-energy transduction. *Phys. Rev. A* **1989**, *39*, 6416–6435.

(64) Astumian, R. D. Kinetic asymmetry allows macromolecular catalysts to drive an information ratchet. *Nat. Commun.* **2019**, *10*, 3837.

(65) Penocchio, E.; Ragazzon, G. Kinetic Barrier Diagrams to Visualize and Engineer Molecular Nonequilibrium Systems. *Small* 2206188.

(66) Marchetti, T.; Roberts, B. M. W.; Frezzato, D.; Prins, L. J. A Minimalistic Covalent Bond-Forming Chemical Reaction Cycle that Consumes Adenosine Diphosphate. *Angew. Chem. Int. Ed. n/a*, e202402965.

(67) Leanza, L.; Perego, C.; Pesce, L.; Salvalaglio, M.; von Delius, M.; Pavan, G. M. Into the dynamics of rotaxanes at atomistic resolution. *Chem. Sci.* **2023**, *14*, 6716–6729.

(68) Steudel, F. M.; Ubasart, E.; Leanza, L.; Pujals, M.; Parella, T.; Pavan, G. M.; Ribas, X.; von Delius, M. Synthesis of C60/[10]CPP-Catenanes by Regioselective, Nanocapsule-Templated Bingel Bis-Addition. *Angew. Chem. Int. Ed.* e202309393.

(69) Albaugh, A.; Gingrich, T. R. Estimating reciprocal partition functions to enable design space sampling. *J. Chem. Phys.* **2020**, *153*, 204102.

(70) Albaugh, A.; Gu, G.; Gingrich, T. R. Sterically driven current reversal in a molecular motor model. *Proc. Natl. Acad. Sci. U.S.A.* **2023**, *120*, e2210500120.

(71) Albaugh, A.; Fu, R.-S.; Gu, G.; Gingrich, T. R. Limits on the Precision of Catenane Molecular Motors: Insights from Thermodynamics and Molecular Dynamics Simulations. *J. Chem. Theory Comput.* **2024**, *20*, 1–6.

(72) Amano, S.; Esposito, M.; Kreidt, E.; Leigh, D. A.; Penocchio, E.; Roberts, B. M. W. Insights from an information thermodynamics analysis of a synthetic molecular motor. *Nat. Chem.* **2022**, *14*, 530–537.

(73) Astumian, R. D. Nonequilibrium steady states, ratchets, and kinetic asymmetry. *Matter* **2023**, *6*, 533–2536.

(74) Burbaum, J. J.; Raines, R. T.; Albery, W. J.; Knowles, J. R. Evolutionary optimization of the catalytic effectiveness of an enzyme. *Biochem.* **1989**, *28*, 9293–9305.

(75) Penocchio, E.; Bachir, A.; Credi, A.; Astumian, R. D.; Ragazzon, G. Analysis of kinetic asymmetry in a multi-cycle chemical reaction network establishes the principles for autonomous compartmentalized molecular ratchets. *ChemRxiv* **2024**, *n/a*, n/a.